The roles of dystrophin and dystrobrevin : in synaptic signaling in drosophila

Potikanond, S.

CHAPTER 4

The Pre- and Postsynaptic roles of Dystroglycan at the *Drosophila* Neuromuscular Junction

The Pre- and Postsynaptic Roles of Dystroglycan at the *Drosophila* Neuromuscular Junction are Played by Distinct Protein Isoforms

Saranyapin Potikanond, Gonneke S. K. Pilgram, Anja W.M. de Jong, Lee G. Fradkin, and Jasprina N. Noordermeer

Laboratory of Developmental Neurobiology, Department of Molecular and Cell Biology, Leiden University Medical Center, Einthovenweg 20, P.O. Box 9600, 2300 RC Leiden, The Netherlands

Abstract

Dystroglycan has been shown to physically interact with Dystrobrevin via Dystrophin to form the core of the Dystrophin Glycoprotein complex. In this report, we show that Dystroglycan is required for localizing both Dystrophin and Dystrobrevin to the postsynaptic region of the synapse which supports the existence of a Dystrophin Glycoprotein complex at the *Drosophila* neuromuscular junction. Furthermore, we demonstrate that the absence of Dystroglycan, either pre- or postsynaptically, suppresses the increased neurotransmitter release at the $Dys^{DLP2\ E6}$ and the Dyb^{11} mutant NMJs. *Dystroglycan* mutants display ultrastructural synaptic defects, specifically significantly reduced levels of Synaptotagmin and increased CaMKII expression. Together, these data begin to parse out the different roles of Dystroglycan, Dystrobrevin and Dystrophin at the neuromuscular junction.

Introduction

Dystroglycan (DG) is a transmembrane protein that forms the basis of the DGC's link between extracellular matrix and the actin cytoskeleton. In mammals, DG is encoded by the single gene *DAG1* which consists of two exons and an intron. DG is post-translationaly cleaved into two fragments, α-DG and β-DG. α-DG is located at the extracellular surface where it binds to laminin2, agrin, perlecan and neurexin ([1], [2]). In *Drosophila*, there are three different protein isoforms which arise from alternative splicing of the primary transcript, *Dg-RA*, *Dg-RB* and *Dg-RC*, leading to three polypeptides; DG-A, DG-B and DG-C [3]. DG-C is the longest isoform and contains a mucin-like domain. This domain is important for binding to Laminin [4]. DG-C is predominantly expressed in embryonic axons [3]. The DG isoforms that lack the mucin-like domain, DG-A and DG-B, are required to maintain polarity in the follicular epithelium [5], suggesting that these isoforms likely have different roles in different tissues in *Drosophila*. Although DG is part of the DGC, the *Dg* mutant neuromuscular (NMJ) phenotype is different from those of the *Dyb* and *Dys* mutants. The absence of DG leads to decreased neurotransmitter release ([6], [7]), while the absence of *Dys* [8] or *Dyb* (**Chapter 3.1**) causes increased neurotransmitter release. Here, we present an evaluation of the interactions of *Dg* and *Dyb* at the NMJ and have begun a dissection of possible pre- versus postsynaptic roles of DG.

Material and Methods

Fly stocks

w^{1118} served as the wild type control genotype for stainings, electrophysiology and transmission electron microscopy analyses. The generation of the Dyb^{11} mutant line was described (**Chapter**

3.1). Dg^{p} (PBac{RB}Dge01554) is a hypomorphic allele of *Dg* , the Piggybac element insertion in *Dg* leads to a 90% decrease in the transcription of all DG-encoding isoforms [6]. A deficiency uncovering *Dg*, "Df (Dg)" (Df(2R)ED2457) was obtained from the Bloomington *Drosophila* Stock Center. The *Dys* DLP2 isoform null mutant allele, Dys^{DLP2E6}, was described previously [8]. To minimize possible genetic background effects, we backcrossed each allele against wild type control flies for at least 5 generations prior to using them in electrophysiological analyses. The following GAL4 driver lines were used: 24B-GAL4 [9], G14-GAL4 [10], Mhc-GAL4 [11] and OK6-GAL [10].

Immunohistochemistry

3rd instar larvae were dissected and fixed in solutions that were optimized for particular antibodies. For DG staining, third instar larvae were dissected in cold HL3 (70 mM NaCl, 5 mM 20 mM KCl, 10mM $NaHCO_3$, 5 mM Trehalose, 115 mM Sucrose 115 and 5mM BES/HEPES) and fixed in Bouin's fixative [12] for 15 minutes. For others antibody labelings, samples were dissected in cold PBS and body walls were fixed in 4% formaldehyde in PBS, washed in PBS and then incubated with primary antibody overnight at 4° C followed by application of secondary fluorescent antibody for 1.5 hrs, subsequent washing and mounting in 0.1% Triton X in PBS. Body wall synapses were visualized by confocal microscopy (Leica TCS SL, Leica Microsystems, Heidelberg, Germany). Primary antibodies used were anti-HRP-FITC (Promega, Madison, WI) 1:500, rabbit anti-DYBCO2H; **Chapter 3.1**) 1:2500, rabbit anti-DYS (a gift from Andreas Wodarz, [13]) 1:1000, rabbit-anti-Dp186 [14], rabbit anti-DG (SN1420; our unpublished antiserum) 1:2500, mouse anti-synapsin 1:1000 ([15], DHSB), mouse anti-GluRIIA ([16]; Developmental studies Hybridoma Bank (DSHB), University of Iowa, Iowa) rabbit anti-GluRIIB ([7]; a kind gift from A. DiAntonio), mouse anti-Fas2 (1D4; [17]) 1:100, anti-mouse discs-large ([18]; DSHB) 1:10000, mouse anti-Bruchpilot (nc82 mAb) ([19]; DHSB) 1:50, rabbit anti-CaMKII (1:2500; [20], a kind gift from L. Griffith) and anti-Synaptotagmin (1:500; [21]; DSHB).

Imaging and quantified intensity of protein at NMJ

Labeled 3rd larval body walls were visualized on a confocal microscope (Leica SL) and laser power, gain settings and magnification were kept constant to allow comparison of the samples. The intensity of each bouton area was measured as relative fluorescent intensity scale from 0 to maximal 250.

Western blotting of larval body walls

Twelve 3rd instar larval body walls of each were dissected in cold PBS and snap frozen in liquid nitrogen with 30 µl of lysis buffer (50 mM Tris-HCl, pH 8.0, 1% Triton-X100 and 1 tablet of protease inhibitor, added just before used). The samples were homogenized on ice and an equal volume of 2X gel electrophoresis sample buffer was added. Samples were boiled for 5 min and centrifuged at 13K x g for 3 min. Standard SDS-PAGE and immuno-blotting was performed. Rabbit anti-DYBMID (1:10,000), Rabbit anti-DYS (Andreas Wodarz ref; 1:10,000) and mouse anti-actin (MP Biomedicals, Aurora, OH, 1:10K), HRP-conjugated secondary antibodies (Jackson immune research) and chemi-luminiscent detection reagents, ECL Plus (Roche) were used to visualize the proteins.

Transmission electron microscopy

Larval dissection, fixation, embedding, and sectioning were performed as described [8]. Semi-serial sections of w^{1118}, and Df (Dg)/Dg^{p} mutant body walls were prepared and electron micrographs were made of Type Ib boutons on muscles 6/7 using a transmission electron microscope (Tecnai 12 Biotwin, FEI, Eindhoven, The Netherlands).

Electrophysiology

Electrophysiological recordings were performed as described [8].

Statistical analyses

The program GraphPad Prism version 5 was used for statistical analysis. One way ANOVA was performed with least significant differences (LSD) or Bonferroni for post hoc multiple comparisons for statistical analyses. Differences were considered significant when $p<0.05$. *, ** and *** serve as $p\leq 0.05$, $p\leq 0.01$ and $p\leq 0.001$, respectively.

Results and Discussion

Localization of DG at the NMJ

We generated antisera recognizing epitopes in DG common to all isoforms. Staining of 3rd larval instar body walls with anti-DG reveals that DG is present throughout the muscle and is particularly enriched at synaptic boutons (**Fig. 1A**). DG is present both pre- and postsynaptically at the bouton as evidenced by high magnification visualization of boutons co-labeled with anti-DG and the presynaptic marker anti-horseradish peroxidase [22] (**Fig. 1C**). Previously, DG was shown to be present predominantly in the postsynaptic compartment [6]. However, we find that DG is present both at the pre- and postsynaptic compartments. The difference in these reports may be due to the observation that our DG antibody recognized all spliced isoforms while the authors of the other study used anti-DG^{ex8} that detects only DG-C [3].

DG is required for correct localization of the DYS and DYB proteins at the NMJ

In mammals, DG, DYS and DYB form a Dystrophin Glycoprotein Complex (DGC) at the NMJ. Drosophila body walls were examined to ascertain potential similar interactions at the *Drosophila* NMJ (**Fig. 2**). Null alleles of *Dg* do not survive until the 3rd larval instar, and Dystroglycan deficiency Df (*Dg*), (Df(2R)ED2457), is similarly early homozygous lethal. Therefore, to evaluate the effects of reduced levels of DG at the 3rd larval instar stage, we used a transheterozygous combination of a *Dg* hypomorph (the PBac{RB}Dge01554 insertion) and Df (*Dg*) which from this point on will be called the *Dg* mutant [Dg^{p}/Df(*Dg*)]. We found that DYS, DYB and DG colocalize at the *Drosophila* NMJ in the wildtype animals (**Fig. 2A-C**). However, DYS and DYB proteins show a significantly reduced expression level at the *Dg* mutant synaptic boutons (**Fig. 2D and E and Suppl. Fig. 1**), indicating that DG is required for the normal DYS and DYB expression patterns at the synapse. Anti-HRP staining revealed apparently wild type structure of the NMJ (data not shown). Interestingly, western blot analyses of *Dg* mutant body wall proteins revealed that they have wild type levels of the DYS and DYB proteins (**Fig. 2G**), suggesting that DYS and DYB are delocalized from the synapses, while the overall levels of these proteins in the muscle fiber are not affected.

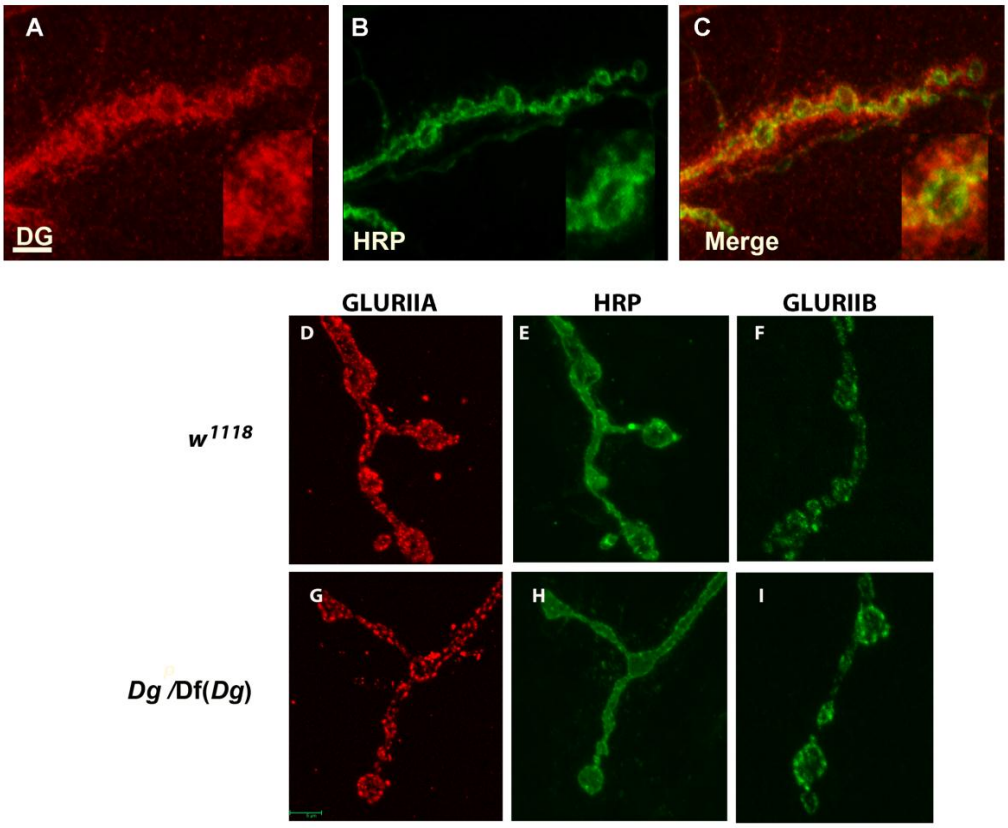

Figure 1. DG is expressed both pre- and postsynaptically at the larval NMJ. DG staining of wild type (**A**) and the presynaptic marker HRP (**B**) and the merge (**C**) are shown. There are no apparent changes DGluRIIA, DGluRIIB and HRP staining, w^{1118} (**D-F**) and *Dg* mutant (**G-I**) are shown. Scale bar = 5 µm.

The absence of DG suppresses the increased neurotransmitter release observed in the *Dys* and *Dyb* mutants

Previously, we reported that a mutation of either *Dyb* or *Dys* has similar effects on the NMJ leading to increased neurotransmitter release. In contrast, a mutation in *Dg* results in decreased neurotransmitter release as determined from calculation of the quantal content (QC) ([6], [7] (**Suppl. Figs. 2 and 3**)). As shown above, DYS and DYB are delocalized from the synapse in the *Dg* mutant without decreases in their overall expression levels (**Fig. 2**). Why do the *Dg* mutants not display a similar increased neurotransmitter release as observed in the *Dyb* and *Dys* deficiencies? To start answering this question, we first ascertained whether there were any changes in the glutamate receptor fields of these mutants but did not find any changes (**Fig. 1G-I**). We also checked if there is an alteration in the bouton numbers but we did not observe obvious changes. However, the number of vesicle release sites (T-bars) was increased in the *Dg* mutant (**Sup. Fig.4**). Interestingly, we found that the pre- or postsynaptically reduced DG levels in the $Dys^{DLP2\ E6}$ or Dyb^{11} mutant backgrounds suppress the increased QC in both the *Dys* and the *Dyb* mutants (**Fig. 3**). The diminished quantal content may result from a general disruption of the synaptic machinery (presynaptic role) or the inhibition of retrograde signaling (postsynaptic role), or both.

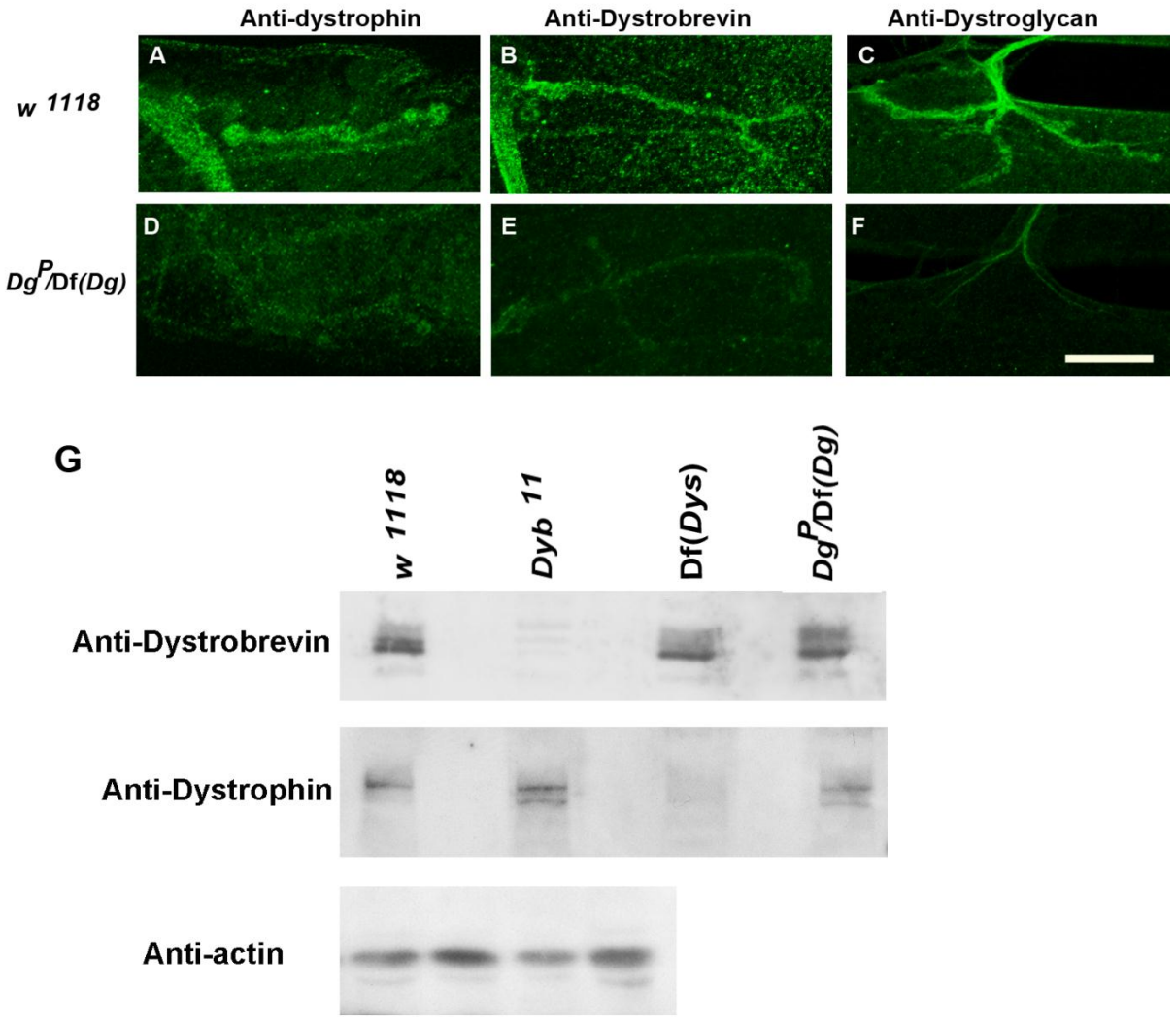

Figure 2. **DYB and DYS are mislocalized in *Dg* mutant.** Anti-DYBCO_2H, anti-DYS and anti-DG antibodies were used to evaluate protein expression in larval body walls and at the NMJ of w^{1118} (**A-C**) and the *Dg* (Dg^P/Df(D^f)) mutants (**D-F**). (**G**) is an immunoblot of larval body wall lysate proteins labeled with anti-DYBCO_2H and anti-DYS. Anti-actin was used as loading control. Note that DYB and DYS protein levels do not change in *Dg* mutants. The scale bar in (F) for (A-F) represents 10 µm.

Possible presynaptic role of Dystroglycan

Our electrophysiological analyses show that DG is required both pre- and postsynaptically for synaptic homeostasis (**Suppl. Fig. 2**). In contrast, previous work [6] showed that reductions in the postsynaptic DG levels by transgenic RNA interference, but not presynaptic levels, result in decreased quantal content. However, rescue experiments to confirm whether DG is indeed required only postsynaptically were not presented in that study [6]. These RNA interference (RNAi) experiments were performed using a pan-neuronal driver (Elav-GAL4) which would also lead to reduction in DG levels at upstream synapses such as those between an interneuron and the motoneuron, therefore complicating the interpretation of the phenotype. We therefore performed RNAi presynaptically using a motoneuron driver (OK6-GAL4) and rescue experiments using transgenes encoding the two different DG splice forms. We found that UAS-*Dg-RC*, which is normally predominantly expressed in axons, rescued the *Dg* mutant quantal content phenotype when expressed presynaptically (**Fig. 4**). Moreover, presynaptic expression of DG-C resulted in quantal content levels significantly above background. This can possibly be explained by the results from our localization studies (**Fig. 2**). DYB and DYS were seen to be

mis-localized in *Dg* mutant. If DG is restored in presynaptic compartment only, DYB and DYS will likely still not be properly re-localized in the postsynaptic compartment leading to a *Dyb*/*Dyb* mutant-like quantal content phenotype

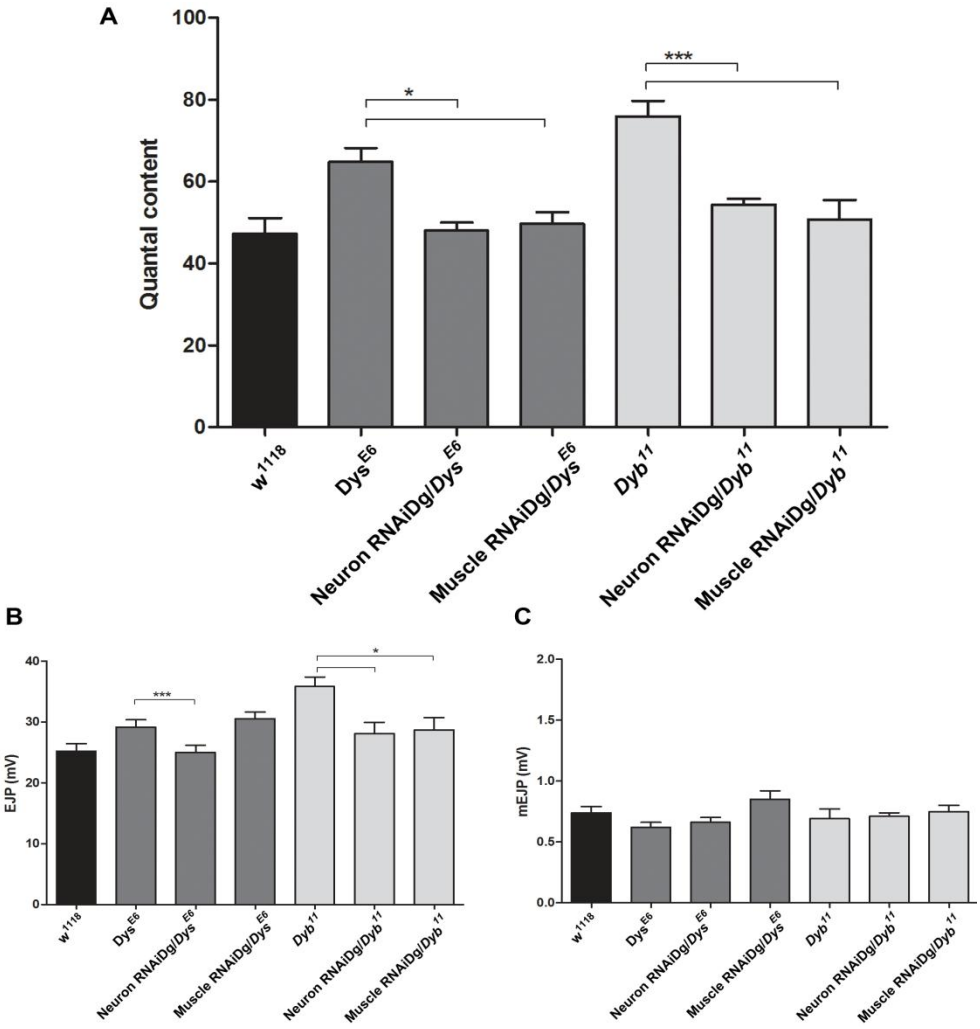

Figure 3. Decreased DG levels block the increased presynaptic neurotransmitter release in the *Dyb* and *Dys* mutants. A bar graphs show quantal contents (**A**), EJP (**B**) and mEJP (**C**) of the w^{1118}, Dys^{E6} (Dys^{E6}*w^{1118}), Neuron RNAiDg/Dys^{E6} (OK6-GAL4;Dys^{E6}*RNAiDg), Muscle RNAiDg/Dys^{E6} (G14-GAL4;Dys^{E6}*RNAiDg), Dyb^{11}(Dyb^{11}*w^{1118}), Neuron RNAiDg/Dyb^{11}(OK6-GAL4;Dyb^{11}*RNAiDg), Muscle RNAiDg/Dyb^{11}(G14-GAL4; Dyb^{11}*RNAiDg). All measurements were performed at 0.6 mM Ca^{2+}.

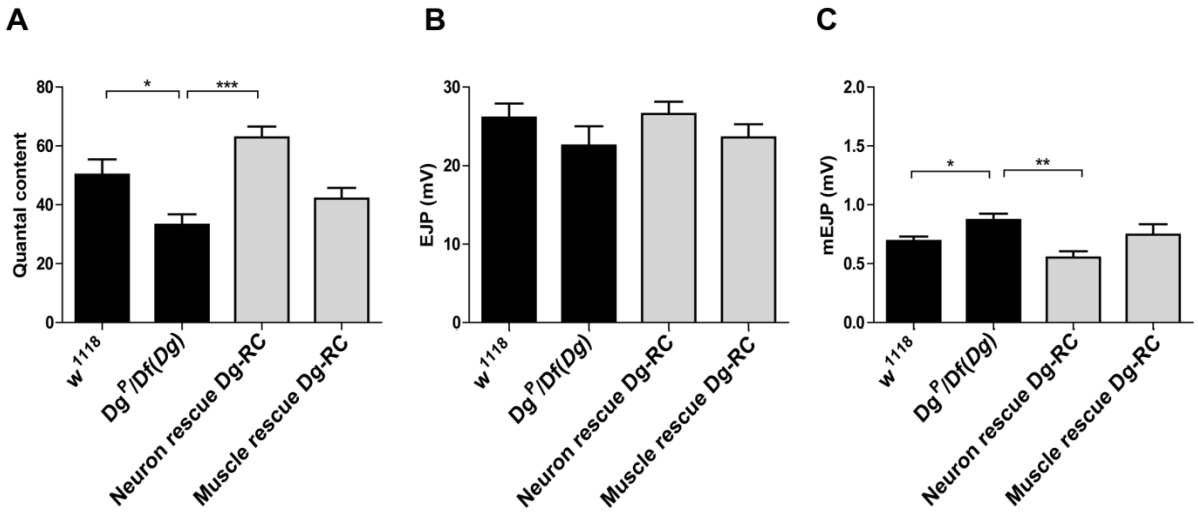

Figure 4. Presynaptic rescue of the Dg mutant neurotransmitter release phenotype by the DG-C isoform. The bar graphs display the quantal content (**A**), mEJP amplitudes (**B**) and EJP amplitudes (**C**) of the indicated genotypes.

The bouton ultrastructure is altered in the *Dg* mutant.

In addition to *Dg* having a presynaptic role, *Dg* mutants showed presynaptic ultrastructural defects. The postsynaptic muscle membrane folds around individual boutons at the *Drosophila* NMJ. This structure is called the subsynaptic reticulum (SSR). Many proteins shown to be relevant for the proper functioning of the NMJ, for example, the N-CAM homolog Fasciclin II (FasII) [23] and the PSD95 homolog discs large (DLG) [24], localize to the SSR.

In wild type boutons, the SSR area is well-organized and characteristically shaped (**Fig. 5A**). *Dg* mutants display increased numbers of T-bars, presynaptic structures thought to be vesicle docking sites [25]. The mutant presynaptic density also shows signs of detachment from postsynaptic density (PSD), a phenotype rarely seen in wild type (**Fig. 5D**). Furthermore, the SSR is significantly thinner than wild type (**Fig. 5B**). Giant vesicles (**Fig. 5C**) were present in 62% of the boutons in *Dg* mutant versus 33% in controls, indicating alterations in the loading of neurotransmitter into vesicles in the mutant. Overall bouton shape and the active zone length in the mutant were not different from the wild type control animals. Despite these obvious changes in both pre- and postsynaptic ultrastructure, we did not observe altered FasII and DLG expression patterns in the *Dg* mutants (data not shown).

Synaptotagmin expression is reduced in the *Dg* mutant

The levels of Synaptotagmin-1 (Syt-1), a synaptic vesicle protein known to interact with phosphoinositol-2-phosphate [PI(4,5)P_2], also known as PIP_2 [26–29], appear to be decreased in the *Dg* mutant (**Fig. 6**). Syt-1 is a major Ca^{2+} sensor that rapidly catalyzes Ca^{2+}-dependent secretion of neurotransmitters (reviewed in [30]). It has been reported that *Drosophila Syt* mutants show decreased neurotransmitter release resulting from smaller evoked synaptic potential with increased the frequency ([31], [32]). The decrease neurotransmitter release in *Dg* mutant is therefore possibly caused by the observed decrease in SYT levels. Furthermore, reduction of SYT-1 levels may alter the function of PIP_2 which is a phospholipid component concentrated at the plasma membrane of most cells, including neurons. PIP_2 plays a regulatory roles in vesicle recycling which are important for synaptic transmission [33–37]. Alterations in

the amounts or distribution of PIP_2 may disturb several steps in the recycling of synaptic vesicles. In support of this hypothesis, a newly characterized synaptic protein,

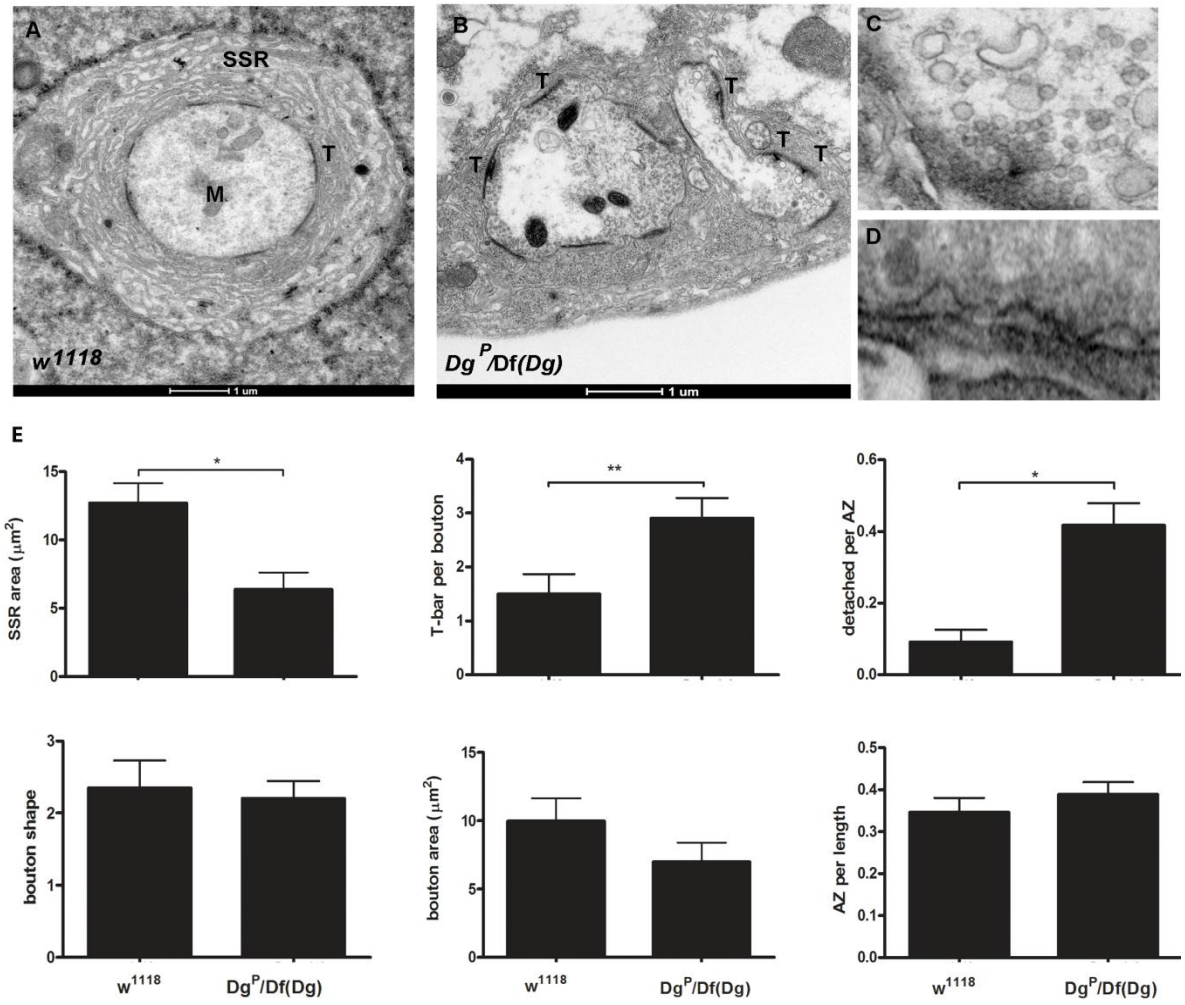

Figure 5. Ultra-structural defects are observed at the *Dg* mutant NMJ. 3rd instar larval body walls were prepared by ultrathin sectioning and the muscle 6 and 7 synapses were visualized by electron microscopy. Representative type Ib bouton in a wild type control (w^{1118}) and *Dg* mutant (Dg^P/Df(*Dg*)) are shown (**A** and **B**). SSR= subsynaptic reticulum, M= mitochondria, T= T-bar. A giant vesicle is shown in **C**. Zoom in detached region of the synaptic membrane is shown in **D.** The bar graphs show the mean of SSR, T-bar per active zone, detached of synaptic membrane per active zone, Bouton shape, SSR area and AZ per length as indicated in each graph are shown in **E**. *, ** are $p \leq 0.05$, $p \leq 0.01$, respectively. 3-5 different larval body walls were analyzed. The numbers of bouton analyzed were 18 in w^{1118} and 22 in *Dg* mutant.

Tweek, affects the PIP_2 pools at the synapse; *Tweek* mutants have reduced PIP_2 at the synapse. The mutants have a similar phenotype as the *Dg* mutant: an increase in quantal size, the presence of giant vesicles (**Fig. 5C**) and a decrease in neurotransmitter release [38].

Another synaptic protein, Neurexin, may also play a role in causing the defect of neurotransmitter release in the *Dg* mutant. Mammalian DG has been shown to bind Neurexin in the brain [1]. Neurexin is a synaptic vesicle protein that serves as a presynaptic adhesion molecule maintaining the pre/postsynaptic interface by binding with its postsynaptic partner, Neuroglin [39]. *Neurexin* (*Nrx-1*) mutants also exhibit presynaptic membrane detachment at the *Drosophila* NMJ (same as **Fig. 5D**), an increase of mEJPs, an increased numbers of T-bars and reduced quantal content. However, the *Nrx-1* mutant NMJ displays decreased bouton counts while there is no change in bouton number in the *Dg* mutant (**Suppl. Fig. 4**) [40]. Taken

together, the decrease in the neurotransmitter release in the *Dg* mutants may be caused by possible defects in the vesicle release machinery mediated by Nrx-1, PIP_2 and SYT-1.

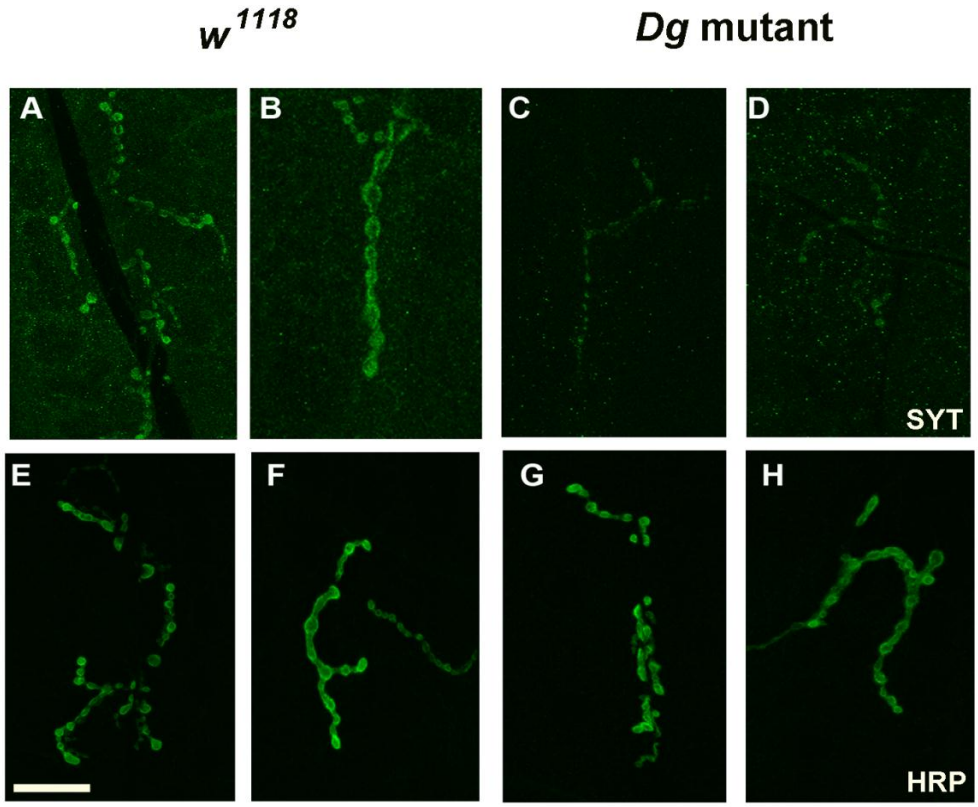

Figure 6. Synaptotagmin expression was reduced in *Dg* mutant. 3rd instar larval body walls were labeled with anti-synaptotagmin in w^{1118} (**A** and **B**) and the *Dg* mutant (**C** and **D**) at muscles 6/7 and muscle 4, respectively. Anti-HRP was used to label bouton of w^{1118} (**E** and **F**) and *Dg* mutant (**G** and **H**) at muscle 6/7 and muscle 4, respectively. Scale bar = 30 μm.

Postsynaptic roles of DG

Reduction of the DG levels in the postsynaptic compartment was previously shown to lead to a decrease in neurotransmitter release ([6], [7]). Above, we have shown that the *Dg* mutant decreased QC phenotype was rescued by presynaptic expression of the Dg-RC protein. We performed similar synapse-side-specific rescue experiments with the Dg-RB transgene and found, surprisingly that it also rescued the Dg mutant phenotype, however, when expressed postsynaptically but not presynaptically (**Fig.** 7). This is in contrast to the case of Dg-RC and suggests that the two isoforms play roles at opposing sides of the NMJ.

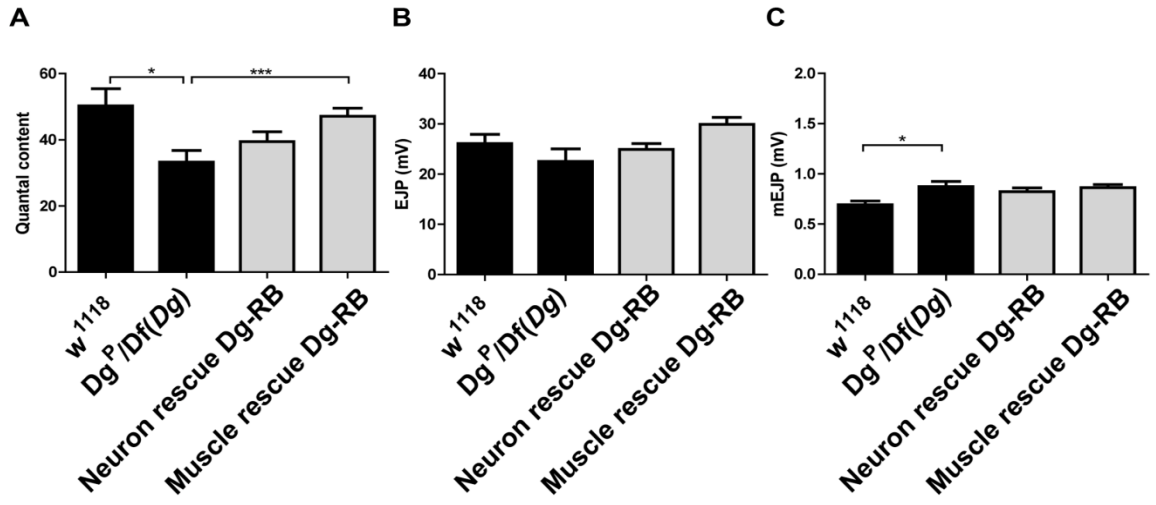

Figure 7. **Postsynaptic expression of the *Dg-RB* isoform rescues the Dg mutant quantal content phenotype.** Bar graph representations of mean ± SEM values of quantal content (**A**), EJP amplitudes (**B**) and mEJP (**C**) are shown. All measurements were performed at 0.6 mM Ca^{2+}. * and *** are $p \leq 0.05$ and $p \leq 0.001$.

CaMKII expression is significantly elevated in the *Dg* mutant

We have inferred the existence of a retrograde signaling pathway to explain how the absence of postsynaptic DYS [8] or DYB (**Chapter 3.1**) exerts it effects on presynaptic function and morphology. The effects of reduced DG levels on neurotransmitter release may possibly reflect the blocking of this retrograde pathway. One molecule that we have implicated in the DYS/DG pathway is the Calcium/calmodulin-dependent protein kinase II (CaMKII), a ubiquitously expressed serine/threonine protein kinase. Mutation of the *CaMKII* gene or inhibition of CaMKII by expressing a peptide that blocks kinase function in *Drosophila* was shown to impair larval neuromuscular transmission ([41], [42]). The ultrastructural defect, an underdeveloped SSR, which we observe in the *Dg* mutant, is very similar to that seen when constitutively-active CaMKII is postsynaptically expressed (**Fig. 3C** of [43]). Interestingly, we observe an increased level of CaMKII at the *Dg* NMJ (**Fig. 8**). Increased CaMKII levels in the *Dg* mutant may block retrograde signaling leading to a prevention of the increase in the neurotransmitter release in the *Dyb* and *Dys* mutant backgrounds.

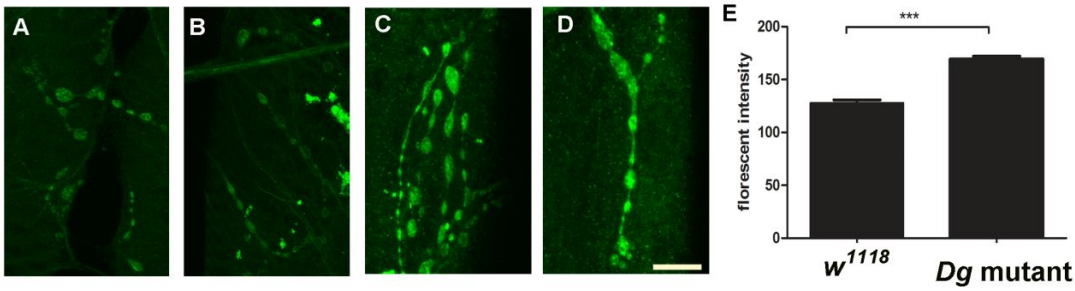

Figure 8. CaMKII expression is significantly elevated in the Dg mutant. Anti-CaMKII was used to stain 3rd instar body wall of w^{1118} (**A** and **B**) and *Dg* mutant (**C** and **D**) at muscle 6/7 and muscle 4, respectively. The images were taken by a Leica confocal SL with the same parameter settings. The boutons from abdominal segment 2-5 were analyzed in a form of relative fluorescent intensity and shown as histogram in **E**. Total number of bouton count was 231 and 244 for w^{1118} and *Dg* mutant, respectively. Scale bar = 15 µm.

Conclusions

In this chapter we have presented further evidence for the existence of a DGC complex at the Drosophila NMJ. The central component, DG, is required for the correct synaptic localization of DYB and DYS. The pre- and postsynaptic roles of DG seem to be played by distinct isoforms. The reduction of neurotransmitter release observed in the *Dg* mutant is likely caused by improper vesicle release, inappropriate retrograde signaling, or a combination thereof. Alterations in the levels of synaptic proteins such as SYT-1 and NRX-2 may underlie the abnormal vesicle release observed at the *Dg* mutant NMJ. Furthermore, the ultrastructure of the *Dg* mutant bouton was abnormal; an underdeveloped SSR, giant vesicles and detachment of synaptic membrane, similar to that observed when CaMKII is inhibited postsynaptically. Thus, the increased levels of CaMKII in the DG mutants may be contributing to a reduction in retrograde signaling. In combination, these pre- and postsynaptic defects at the DG mutant NMJ will lead to reduced synaptic transmission, but the exact mechanisms of DG function will require further study.

References

[1] S. Sugita, F. Saito, J. Tang, J. Satz, K. Campbell, and T. C. Sudhof, "A stoichiometric complex of neurexins and dystroglycan in brain," *J Cell Biol*, vol. 154, no. 2, pp. 435-445, 2001.

[2] G. S. Pilgram, S. Potikanond, R. A. Baines, L. G. Fradkin, and J. N. Noordermeer, "The roles of the dystrophin-associated glycoprotein complex at the synapse," *Mol Neurobiol*, vol. 41, no. 1, pp. 1-21.

[3] M. Schneider and S. Baumgartner, "Differential expression of Dystroglycan-spliceforms with and without the mucin-like domain during Drosophila embryogenesis," *Fly (Austin)*, vol. 2, no. 1, pp. 29-35, 2008.

[4] M. Kanagawa et al., "Molecular recognition by LARGE is essential for expression of functional dystroglycan," *Cell*, vol. 117, no. 7, pp. 953-964, 2004.

[5] W. M. Deng et al., "Dystroglycan is required for polarizing the epithelial cells and the oocyte in Drosophila," *Development*, vol. 130, no. 1, pp. 173-184, 2003.

[6] L. Bogdanik et al., "Muscle dystroglycan organizes the postsynapse and regulates presynaptic neurotransmitter release at the Drosophila neuromuscular junction," *PLoS ONE*, vol. 3, no. 4, p. e2084, 2008.

[7] Y. P. Wairkar, L. G. Fradkin, J. N. Noordermeer, and A. DiAntonio, "Synaptic defects in a Drosophila model of congenital muscular dystrophy," *J Neurosci*, vol. 28, no. 14, pp. 3781-3789, 2008.

[8] M. C. van der Plas, G. S. Pilgram, J. J. Plomp, A. de Jong, L. G. Fradkin, and J. N. Noordermeer, "Dystrophin is required for appropriate retrograde control of neurotransmitter release at the Drosophila neuromuscular junction," *J Neurosci*, vol. 26, no. 1, pp. 333-344, 2006.

[9] A. H. Brand and N. Perrimon, "Targeted gene expression as a means of altering cell fates and generating dominant phenotypes," *Development*, vol. 118, no. 2, pp. 401-415, 1993.

[10] H. Aberle, A. P. Haghighi, R. D. Fetter, B. D. McCabe, T. R. Magalhaes, and C. S. Goodman, "wishful thinking encodes a BMP type II receptor that regulates synaptic growth in Drosophila," *Neuron*, vol. 33, no. 4, pp. 545-558, 2002.

[11] G. W. Davis, A. DiAntonio, S. A. Petersen, and C. S. Goodman, “Postsynaptic PKA controls quantal size and reveals a retrograde signal that regulates presynaptic transmitter release in Drosophila,” *Neuron*, vol. 20, no. 2, pp. 305-315, 1998.

[12] Bouin Pol Andre, “bouin’s solution,” *Arch. d’Anat. Micr.*, p. 1: 225., 1897.

[13] M. Schneider et al., “Perlecan and Dystroglycan act at the basal side of the Drosophila follicular epithelium to maintain epithelial organization.,” *Development (Cambridge, England)*, vol. 133, no. 19, pp. 3805-15, Oct. 2006.

[14] L. G. Fradkin, R. A. Baines, M. C. van der Plas, and J. N. Noordermeer, “The dystrophin Dp186 isoform regulates neurotransmitter release at a central synapse in Drosophila,” *J Neurosci*, vol. 28, no. 19, pp. 5105-5114, 2008.

[15] B. Michels et al., “Cellular site and molecular mode of synapsin action in associative learning.,” *Learning & memory (Cold Spring Harbor, N.Y.)*, vol. 18, no. 5, pp. 332-44, Jan. 2011.

[16] C. M. Schuster, A. Ultsch, P. Schloss, J. A. Cox, B. Schmitt, and H. Betz, “Molecular cloning of an invertebrate glutamate receptor subunit expressed in Drosophila muscle.,” *Science (New York, N.Y.)*, vol. 254, no. 5028, pp. 112-4, Oct. 1991.

[17] G. W. Davis, C. M. Schuster, and C. S. Goodman, “Genetic analysis of the mechanisms controlling target selection: target-derived Fasciclin II regulates the pattern of synapse formation.,” *Neuron*, vol. 19, no. 3, pp. 561-73, Sep. 1997.

[18] D. Parnas, A. P. Haghighi, R. D. Fetter, S. W. Kim, and C. S. Goodman, “Regulation of postsynaptic structure and protein localization by the Rho-type guanine nucleotide exchange factor dPix.,” *Neuron*, vol. 32, no. 3, pp. 415-24, Nov. 2001.

[19] D. A. Wagh et al., “Bruchpilot, a protein with homology to ELKS/CAST, is required for structural integrity and function of synaptic active zones in Drosophila.,” *Neuron*, vol. 49, no. 6, pp. 833-44, Mar. 2006.

[20] L. C. Griffith, L. M. Verselis, K. M. Aitken, C. P. Kyriacou, W. Danho, and R. J. Greenspan, “Inhibition of calcium/calmodulin-dependent protein kinase in Drosophila disrupts behavioral plasticity,” *Neuron*, vol. 10, no. 3, pp. 501-509, 1993.

[21] M. Yoshihara, Z. Guan, and J. T. Littleton, “Differential regulation of synchronous versus asynchronous neurotransmitter release by the C2 domains of synaptotagmin 1.,” *Proceedings of the National Academy of Sciences of the United States of America*, vol. 107, no. 33, pp. 14869-74, Aug. 2010.

[22] L. Y. Jan and Y. N. Jan, “Antibodies to horseradish peroxidase as specific neuronal markers in Drosophila and in grasshopper embryos.,” *Proceedings of the National Academy of Sciences of the United States of America*, vol. 79, no. 8, pp. 2700-4, Apr. 1982.

[23] C. M. Schuster, G. W. Davis, R. D. Fetter, and C. S. Goodman, “Genetic dissection of structural and functional components of synaptic plasticity. II. Fasciclin II controls presynaptic structural plasticity,” *Neuron*, vol. 17, no. 4, pp. 655-667, 1996.

[24] V. Budnik, “Synapse maturation and structural plasticity at Drosophila neuromuscular junctions.,” *Current opinion in neurobiology*, vol. 6, no. 6, pp. 858-67, Dec. 1996.

[25] R. G. Zhai and H. J. Bellen, “The architecture of the active zone in the presynaptic nerve terminal.,” *Physiology (Bethesda, Md.)*, vol. 19, pp. 262-70, Oct. 2004.

[26] J. Bai, W. C. Tucker, and E. R. Chapman, “PIP2 increases the speed of response of synaptotagmin and steers its membrane-penetration activity toward the plasma membrane.,” *Nature structural & molecular biology*, vol. 11, no. 1, pp. 36-44, Jan. 2004.

[27] G. Schiavo, Q. M. Gu, G. D. Prestwich, T. H. Söllner, and J. E. Rothman, "Calcium-dependent switching of the specificity of phosphoinositide binding to synaptotagmin.," *Proceedings of the National Academy of Sciences of the United States of America*, vol. 93, no. 23, pp. 13327-32, Nov. 1996.

[28] A. Radhakrishnan, A. Stein, R. Jahn, and D. Fasshauer, "The Ca2+ affinity of synaptotagmin 1 is markedly increased by a specific interaction of its C2B domain with phosphatidylinositol 4,5-bisphosphate.," *The Journal of biological chemistry*, vol. 284, no. 38, pp. 25749-60, Sep. 2009.

[29] M. Fukuda, T. Kojima, J. Aruga, M. Niinobe, and K. Mikoshiba, "Functional diversity of C2 domains of synaptotagmin family. Mutational analysis of inositol high polyphosphate binding domain.," *The Journal of biological chemistry*, vol. 270, no. 44, pp. 26523-7, Nov. 1995.

[30] E. R. Chapman, "How does synaptotagmin trigger neurotransmitter release?," *Annual review of biochemistry*, vol. 77, pp. 615-41, Jan. 2008.

[31] A. DiAntonio and T. L. Schwarz, "The effect on synaptic physiology of synaptotagmin mutations in Drosophila.," *Neuron*, vol. 12, no. 4, pp. 909-20, Apr. 1994.

[32] M. Yoshihara and J. T. Littleton, "Synaptotagmin I functions as a calcium sensor to synchronize neurotransmitter release.," *Neuron*, vol. 36, no. 5, pp. 897-908, Dec. 2002.

[33] O. Cremona et al., "Essential role of phosphoinositide metabolism in synaptic vesicle recycling," *Cell*, vol. 99, no. 2, pp. 179-188, 1999.

[34] G. Di Paolo et al., "Impaired PtdIns(4,5)P2 synthesis in nerve terminals produces defects in synaptic vesicle trafficking.," *Nature*, vol. 431, no. 7007, pp. 415-22, Sep. 2004.

[35] T. W. Harris, E. Hartwieg, H. R. Horvitz, and E. M. Jorgensen, "Mutations in synaptojanin disrupt synaptic vesicle recycling," *J Cell Biol*, vol. 150, no. 3, pp. 589-600, 2000.

[36] K. D. Micheva, R. W. Holz, and S. J. Smith, "Regulation of presynaptic phosphatidylinositol 4,5-biphosphate by neuronal activity," *J Cell Biol*, vol. 154, no. 2, pp. 355-368, Jul. 2001.

[37] M. Vicinanza, G. D'Angelo, A. Di Campli, and M. A. De Matteis, "Function and dysfunction of the PI system in membrane trafficking," *EMBO J*, vol. 27, no. 19, pp. 2457-2470, 2008.

[38] P. Verstreken et al., "Tweek, an evolutionarily conserved protein, is required for synaptic vesicle recycling," *Neuron*, vol. 63, no. 2, pp. 203-215, 2009.

[39] C. Dean et al., "Neurexin mediates the assembly of presynaptic terminals.," *Nature neuroscience*, vol. 6, no. 7, pp. 708-16, Jul. 2003.

[40] J. Li, J. Ashley, V. Budnik, and M. A. Bhat, "Crucial role of Drosophila neurexin in proper active zone apposition to postsynaptic densities, synaptic growth, and synaptic transmission.," *Neuron*, vol. 55, no. 5, pp. 741-55, Sep. 2007.

[41] A. P. Haghighi, B. D. McCabe, R. D. Fetter, J. E. Palmer, S. Hom, and C. S. Goodman, "Retrograde control of synaptic transmission by postsynaptic CaMKII at the Drosophila neuromuscular junction," *Neuron*, vol. 39, no. 2, pp. 255-267, 2003.

[42] T. Morimoto, M. Nobechi, A. Komatsu, H. Miyakawa, and A. Nose, "Subunit-specific and homeostatic regulation of glutamate receptor localization by CaMKII in Drosophila neuromuscular junctions.," *Neuroscience*, vol. 165, no. 4, pp. 1284-92, Feb. 2010.

[43] Y. H. Koh, E. Popova, U. Thomas, L. C. Griffith, and V. Budnik, "Regulation of DLG localization at synapses by CaMKII-dependent phosphorylation," *Cell*, vol. 98, no. 3, pp. 353-363, 1999.

Supplemental Figure 1

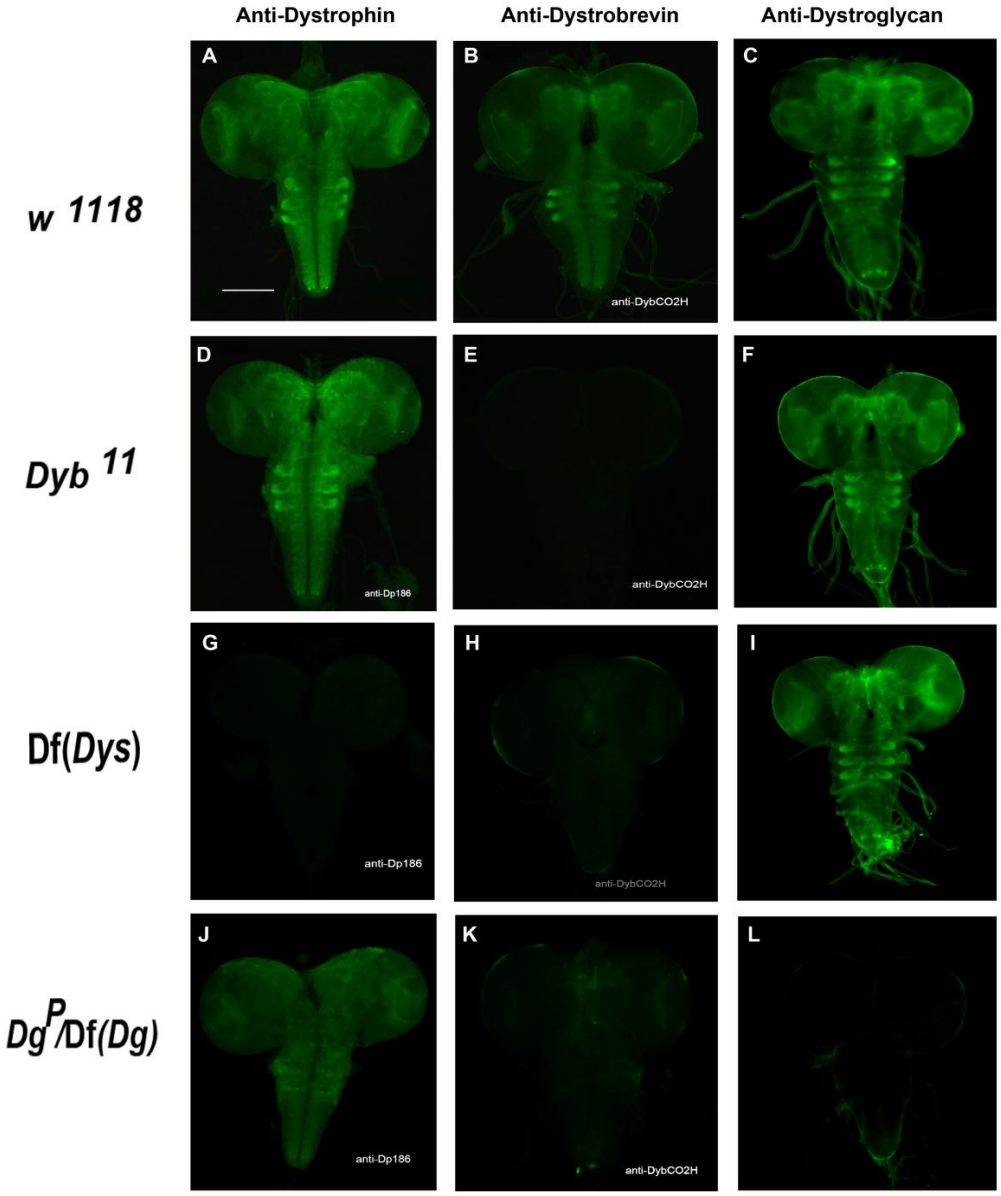

Genotype	Anti-DYB CO_2H	Anti-Dp186	Anti-DG	Anti-Synapsin
w^{1118}	√	√	√	√
Dyb^{11}	X	√	√	√
Df(*Dys*)	X	X	√	√
Dg^{P}/ Df(*Dg*)	less	diffuse	X	√

Supplemental Figure 1. **The mutual interdependence of the localization of the DYB, DYS and DG proteins in the larval central nervous system.** Anti-DybYBCO_2H, anti-Dp186 and anti-DG antibodies were used to evaluate protein expression in the larval brains of w^{1118} (**A-C**), Dyb^{11}) mutant (**D-F**), *Dys* (Df*(Dys)*) mutant (**G-I**), *Dg* (Dg^{P}/ Df*(Dg)*) mutant (**J-L**). The table summarizes protein expression in the brain. √ = present, X= absent. Synapsin antibody was used as a positive control. Scale bar = 100 µm.

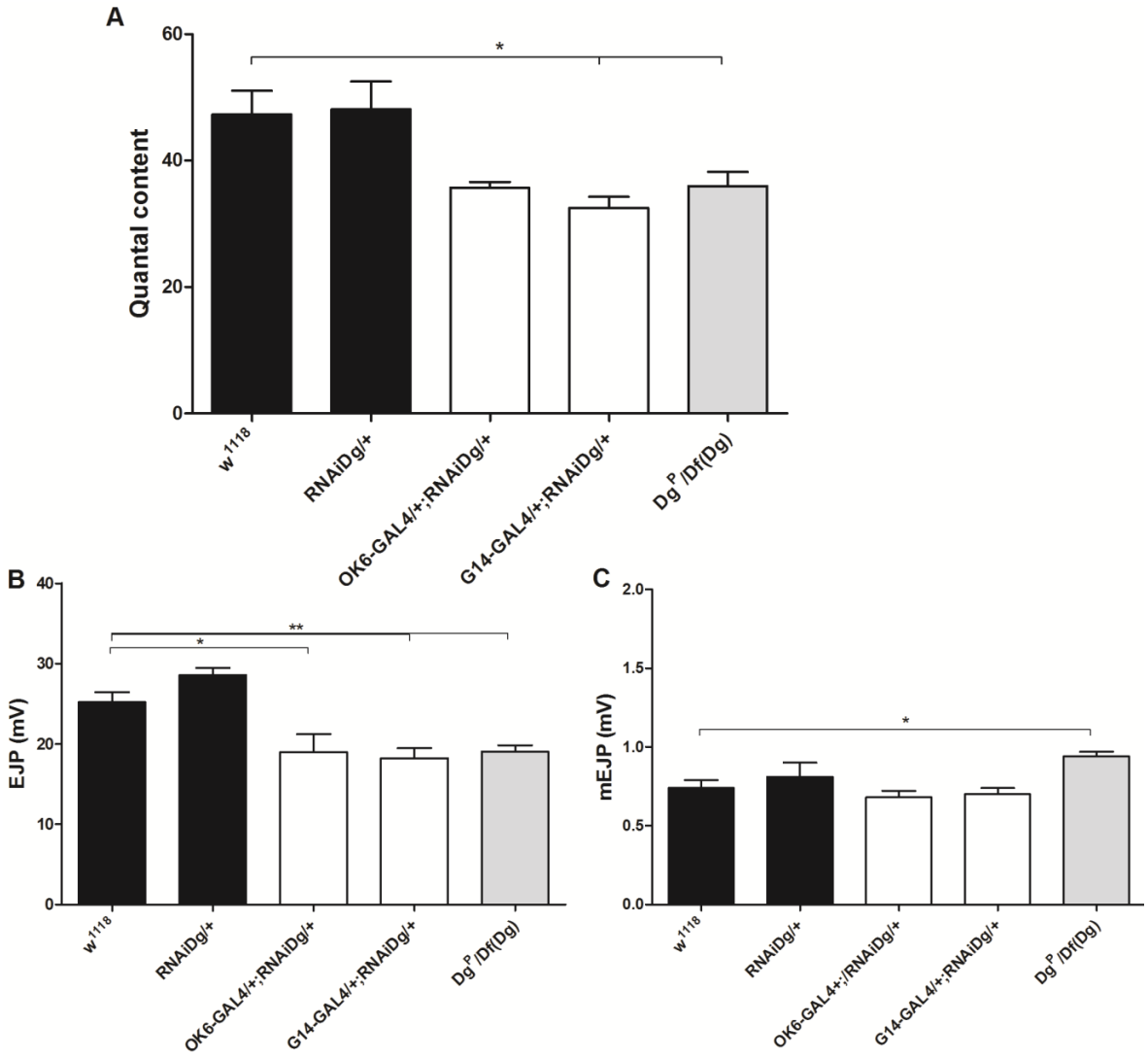

Supplemental Figure 2. **Reduced *Dg* levels in either the pre-or postsynaptic compartment decreased neurotransmitter release levels similarly that that seen in the *Dg* mutant (*Dg*^{P}/Df(*Dg*)).** Bar graph representation of mean ± SEM values of quantal content (**A**), EJP (**B**), mEJP (**C**). All measurements were performed at 0.6 mM Ca^{2+}. * and ** are $p \leq 0.05$ and $p \leq 0.01$.

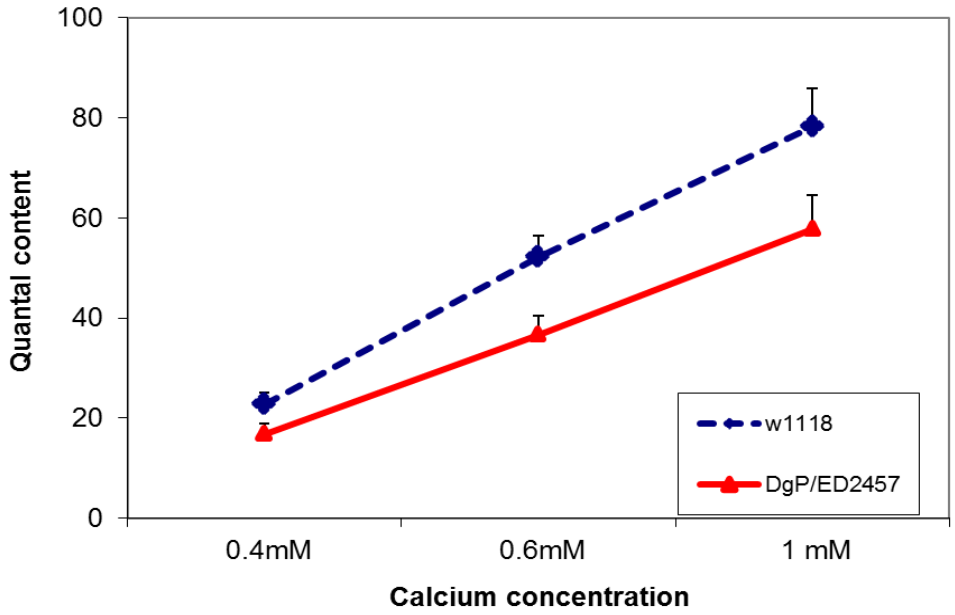

Supplemental Figure 3. Decreased neurotranmitter release in the *Dg* mutant does not depend on Ca^{2+} concentration. Line graphs of quantal content at different Ca^{2+} concentration of w^{1118} (blue line) and the *Dg* mutant (red line) is shown. Ca^{2+} concentrations used are 0.4 mM, 0.6 mM and 1mM.

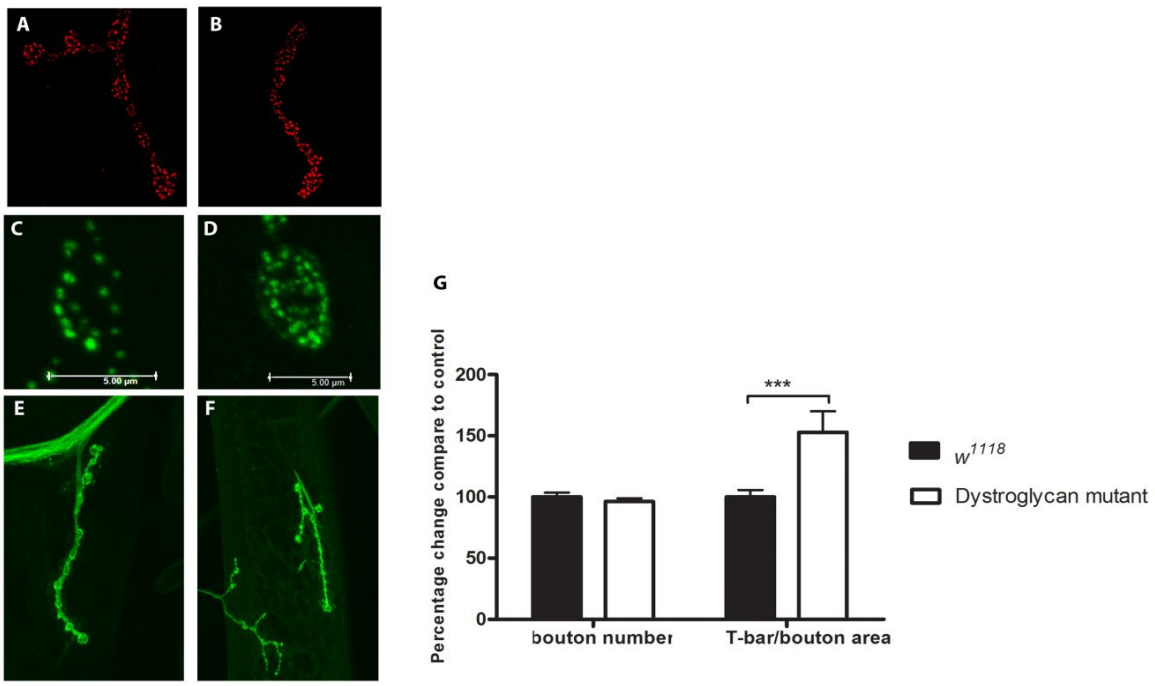

Supplemental Figure 4. The numbers of T-bar are increased in *Dg* mutant. nC82 staining allows the visualization of the number of T-bars at w^{1118} (**A**) and *Dg* mutant (**B**) NMJs. **C** and **D** are high magnified of NC82 staining of single boutons. Anti-HRP staining of w^{1118} and the *Dg* mutant are showed in **E and F**, respectively. The mean of percentage change of bouton number and T-bar per bouton shows in **G**. *** is $p \leq 0.001$. Scale bar = 5 µm.

Supplemental table 1 Average electrophysiological data including fmEJPs, mEJPs, EJPS and QC of all genotypes shown in figures.

Genotype		fmEJP	mEJP	EJP	QC
w^{1118}	Mean SEM* N#	2.66 0.75 14	0.74 0.05 14	25.18 1.28 14	47.29 3.77 14
Dge01554/Df(2R)ED2457 (Dg^{P}/Df(*Dg*))	Mean SEM N	4.61 0.65 19	0.94 0.03 19	19.02 0.79 19	35.93 2.3 19
RNAiDg/+	Mean SEM N	3.52 0.9 9	0.81 0.09 9	28.56 0.09 9	48.1 4.4 9
OK6-GAL4/+;RNAiDg/+	Mean SEM N	2.68 0.38 8	0.64 0.05 8	19 2.2 8	35.72 1.5 8
G14-GAL4/+/RNAiDg/+	Mean Std.Error of Mean N	2.56 0.27 9	0.69 0.04 9	18.22 1.27 9	32.48 1.79 9
Dys^{DLP2E6}	Mean SEM N	2.67 0.38 6	0.62 0.04 6	29.44 1.27 6	64.73 3.5 6
OK6-GAL4/+; *Dys*^{DLP2E6}/RNAiDg	Mean SEM N	3.27 0.3 8	0.66 0.04 8	24.98 1.2 8	47.99 1.93 8
G14-GAL4/+; *Dys*^{DLP2E6}/RNAiDg	Mean SEM N	4.55 0.4 9	0.8 0.07 9	30.5 1.14 9	49.64 1.5 9
Dyb^{11}	Mean SEM N	3.21 0.36 17	0.71 0.04 17	34.58 0.79 17	71.48 6.60 17
Dyb^{11},OK6-GAL4/+ ;RNAiDg/+	Mean SEM N	2.38 0.47 8	0.71 0.03 8	28.66 1.87 8	54.29 1.5 8
Dyb^{11}/+ ;RNAiDg/24B-GAL4	Mean SEM N	1.89 0.45 7	0.75 0.05 7	28.7 2.08 7	50.73 4.72 7
Dg^{P},OK6-GAL4/*Dg*^{P};UASDgRB/+	Mean SEM N	3.98 0.43 14	0.82 0.04 14	24.91 1.21 14	39.43 3.07 14
Dg^{P}/Df(*Dg*); UASDgRB/Mhc-GAL4	Mean SEM N	3.0 0.36 10	0.86 0.03 10	29.96 1.34 10	47.09 62.94 10
Dg^{P},OK6-GAL4/*Dg*^{P}; UASDgRC/+	Mean SEM N	2.49 0.36 7	0.55 0.05 7	26.57 1.57 7	62.94 3.6 7
Dg^{P}/Df(*Dg*); UASDgRC/Mhc-GAL4	Mean SEM N	2.92 0.20 10	0.75 0.09 10	23.6 1.67 10	42.11 3.75 10

* = number of larvae, # = standard error of mean